DOI: 10.3727/096368912X653309

CT-0589 Accepted 03/12/2012 for publication in "*Cell Transplantation*"

THE IMMUNOSUPPRESSIVE EFFECT OF MESENCHYMAL STROMAL CELLS ON B LYMPHOCYTES IS MEDIATED BY MEMBRANE VESICLES

Manuela Budoni*[1], Alessandra Fierabracci*[1], Rosa Luciano*, Stefania Petrini*, Vincenzo Di Ciommo§, Maurizio Muraca*

***Research Laboratories and §Service of Epidemiology and Biostatistics, Children's Hospital "Bambino Gesù" Research Institute, Rome, Italy**

Running title: Mesenchymal stromal cell vesicles inhibit B cells

Correspondence: Prof. Maurizio Muraca
Research Laboratories
Children's Hospital "Bambino Gesù"
Piazza Sant'Onofrio, 4
00165 Rome (Italy)
Tel. +39 06 6859 2210
Fax +39 06 6859 2014
maurizio.muraca@opbg.net

[1]Manuela Budoni and Alessandra Fierabracci equally contributed to this work.

ABSTRACT

The immunomodulatory properties of mesenchymal stromal cells are the subject of increasing interest and of widening clinical applications, but the reproducibility of their effects is controversial and the underlying mechanisms have not been fully clarified.

We investigated the transfer of membrane vesicles, a recently recognized pathway of intercellular communication, as possible mediator of the interaction between mesenchymal stromal cells and B lymphocytes.

Mesenchymal stromal cells exhibited a strong dose-dependent inhibition of B cell proliferation and differentiation in a CpG-stimulated peripheral blood mononuclear cell co-culture system. We observed that these effects could be fully reproduced by membrane vesicles isolated from mesenchymal stromal cell culture supernatants, in a dose-dependent fashion. Next, we evaluated the localization of fluorescent labeled membrane vesicles within specific cell subtypes both by flow cytometry and by confocal microscopy analysis. Membrane vesicles were found to be associated with stimulated B lymphocytes, but not with other cell phenotypes (T lymphocytes, dendritic cells, NK cells), in peripheral blood mononuclear cell culture.

These results suggest that membrane vesicles derived from mesenchymal stromal cells are the conveyors of the immunosuppressive effect on B lymphocytes. These particles should be further evaluated as immunosuppressive agents in place of the parent cells, with possible advantages in term of standardization, safety and feasibility.

Key words: Mesenchymal stromal cells; Membrane vesicles; Immunomodulation; B lymphocytes; Proliferation; Differentiation

INTRODUCTION

Mesenchymal stromal cells (MSCs) have immunomodulatory properties demonstrated *in vitro*, in animal studies and in clinical applications such as the treatment of severe graft versus host disease (GVHD) (4,16,31). However, the underlying mechanisms have not been fully clarified (19,21). In particular, while the suppressive effect of MSCs on activated T cells has been extensively investigated, and found to involve multiple factors (2,17,24), both the effect of MSCs on B cells and the involved mechanisms are more controversial (8,10,22,26,28). Recently, it was demonstrated that several interactions between immune cells are mediated by secreted membrane vesicles (MVs) (27). Various types of secreted MVs have been described, ranging from 50 to 1,000 nm diameter size, exhibiting distinct structural and biochemical properties according to their intracellular site of origin, features probably also affecting their function (5). An increasing body of evidence indicates that they play a pivotal role in cell-to-cell communication (7): in particular, MVs can play a role in intercellular signaling by exchanging mRNA, microRNA, and proteins among cells within a defined microenvironment (29). The aim of this study was to verify the immunomodulatory properties of MVs derived by MSCs (MSC-MVs) on B cell function. Here, we show that the immunosuppressive effect of MSCs on B cells can be reproduced in a dose-dependent fashion by MSC-MVs secreted in the medium by cultured cells.

MATERIALS AND METHODS

MSC culture and expansion

Commercially available bone marrow human MSCs (Lonza, Basel, Switzerland) were plated in 75-cm^2 polystyrene vented tissue culture flasks (Becton Dickinson, USA) at a density of $4x10^3$cells/cm^2 in a volume of 10 ml of Mesencult basal medium (StemCell Technologies, Vancouver, BC, Canada) supplemented with fetal bovine serum (20%, FBS, HyClone Laboratories), 100U/ml penicillin and 100μg/ml streptomycin (Gibco, Grand Island, NY). In order to remove endogenous MVs, FBS was centrifuged overnight at 100,000 x *g* before use. Cultures were incubated at 37°C in a humidified atmosphere containing 5% CO_2. Cells were subsequently maintained in the same medium and passaged at 80-90% confluence in a ratio 1:2 in trypsin/EDTA solution (Invitrogen, Life Technologies, Italy), with the medium changed once a week.

Peripheral blood mononuclear cell isolation

Blood samples from healthy donors were recruited at the Blood Transfusion Center of Children's Hospital Bambino Gesù, Rome. After obtaining informed consent, peripheral blood mononuclear cells (PBMCs) were separated by Ficoll-Hypaque (Histopaque, Sigma-Aldrich Chemical C, St Louis, MO, USA) from 50ml sodium-heparinized venous blood samples, washed twice in Dulbecco's phosphate buffered saline (D-PBS, Euro-Clone, Milan, Italy) and cryopreserved in liquid nitrogen until use. The protocol, involving the use of human material, was approved by the Ethical Committee of the Children's Hospital Bambino Gesù.

Co-culture of PBMCs with MSCs

B cell viability experiments were performed in a co-culture system with MSCs plated in 96-multiwell culture plates (Corning-Costar, Celbio, Milan, Italy) at the initial densities of $2.5x10^4$, $1x10^4$ or $5x10^3$ cells/well in Mesencult basal medium supplemented with FBS (20%). For the immuno-modulation experiments, MSCs were plated in 96-multiwell plates at the concentration of $5x10^3$ cells/well and cultured in Mesencult basal medium supplemented with FBS (20%). On the following day, the medium was aspirated and replaced with PBMCs at $5x10^5$ cells/well, corresponding to a ratio of MSCs/PBMC 1:20, 1:50, 1:100 respectively. In order to evaluate cell proliferation and differentiation, PBMCs had been pre-labeled with 0.5 μM 5-chloromethylfluorescein diacetate (CMFDA, CellTracker; Molecular Probes) according with manufacture's guidelines and co-cultured with MSCs in RPMI 1640 medium (BioWhittaker, Lona, Belgium) supplemented with 10% FBS. B cell stimulation was achieved by incubation with 2.5 μg/ml of human CpG oligodeoxynucleotides 5′-TCGTCGTTTTGTCGTTTTGTCGTT-3′ (Hycult Biotechnology). After one week the co-cultures of PBMCs were rescued, washed in D-PBS, and analyzed by Fluorescent activated cell sorting analysis (FACSCanto II, BD Biosciences).

Co-culture of PBMCs with MSC-MVs

MSC-MVs were isolated with a modification of the procedure of Lamparski *et al* (18). Cultures of MSCs at 90% of confluence were used for the isolation of MVs. The medium from culture plates with $2x10^6$ seeded MSCs was collected at day 5 of culture, and centrifuged at 1,000 x *g* for 20 min to remove the debris. Ten ml of clarified supernatant was concentrated by centrifugation for 20 min at 2,000 x *g* in

sterile hydrated 30 kDa MWCO Amicon Ultra Centrifugal filter (Millipore, Bedford, MA, USA) up to a volume of 15-20 μl. The MSC-conditioned concentrated medium was diluted in 10 ml of PBS in polyallomer tubes (Beckman Coulter, Milan, Italy), then ultra-centrifuged at 100,000 x *g* at 4°C for 1h. At the end of the procedure 2 ml from the bottom of the tubes were collected and concentrated by centrifuging for 20-30 min at 2,000 x *g* in a sterile 30 kDa MWCO Amicon Ultra Centrifugal filter (Millipore) up to a volume of 15-20 µl. MVs were used either undiluted or diluted 1:3, 1:6 in RPMI 1640 (BioWhittaker) and added to $5x10^5$ CMFDA labeled PBMCs 1h and 24h after seeding. After one week in presence of 2.5 μg/ml of human CpG oligodeoxynucleotides additioned at the time of cell seeding, PBMCs were collected by centrifugation, washed and analysed by Flow Cytometry.

Detection of apoptosis

For the detection of apoptosis, PBMCs cultured in medium alone, with CpG or co-cultured with MSC-MVs plus CpG were analyzed by Annexin V and 7-amino-actinomycin (7-AAD) staining. Briefly, after 4 and 7 days in culture, the cells were centrifuged at 300 *g* for 5 min and incubated with anti-CD19 (1:10 phycoerythrin-cyanine 7 [PE-Cy7] conjugated, Becton Dickinson, BD, Franklin Lakes, N.J., USA) for 20 min at 4°C in the dark. After washing with PBS, 5µl of Annexin V (allophycocyanin [APC]-conjugated, BD) and 5µl of vital dye 7-AAD, (peridin-chlorophyll protein complex-conjugated [PerCP], BD) were added in a final volume of 500 µl of Annexin V Binding Buffer 1X (BB1x) according with the manufacture's guideline. After 15 min of incubation in the dark at room temperature, the samples were transferred on fluorescence-activated cell sorting (FACS) tubes (BD) and acquired with a FACS

Canto II (BD). Flow cytometer profiles were analyzed using FACSDiva software (BD). A minimum of 20,000 events were collected per dataset.

Detection of immunoglobulin production

PBMCs were co-cultured in 96-multiwell plates with or without incubation with MSC-MVs in RPMI 1640 (BioWhittaker) supplemented with 10% FBS (Hyclone). After one week the plates were centrifuged at 300 x *g* for 5 min, and the supernatants were collected and tested by enzyme-linked immunosorbent assay (ELISA) in order to assess immunoglobulin production. The 96-multiwell ELISA plates (Corning) were coated with purified goat anti-human IgA or IgG or IgM diluted in PBS and incubated overnight at 4°C (IgA 10µg/ml, IgG 15µg/ml, IgM 2.5µg/ml, Jackson ImmunoResearch Laboratories, West Grove, PA). After three washes in PBS/Tween (0.1%) the supernatants from cell cultures were added to the plates (50 µl/well) and incubated at 37°C for 1h in a humidified atmosphere. After washing, the plates were incubated for 1h at 37°C with 50 µl of peroxidase-conjugated goat anti-human IgA (1:1,000), IgG (1:2,000) or IgM (1:1,000) diluted in PBS (Jackson ImmunoResearch Laboratories). *o*-phenylenediamine tablets (Sigma-Aldrich) diluted in PBS according with manufacture's guideline were used as chromogenic substrate to develop the assay. The reaction was stopped after 30 min by adding 50 µl/well of SDS (10%). At the end of the procedure the plates were red with a microplate spectrophotometer Benchmark Plus at 460 OD.

Flow cytometry

At the end of the experiments, PBMCs were harvested from culture plates, centrifuged at 300 x *g* for 5 min and resuspended in PBS/FBS (2%). Single cell suspensions were incubated in the dark for 20 min at 4°C with directly conjugated

monoclonal antibodies (mAbs) directed against the following human surface molecules: CD19 (1:7 Cy5-conjugated), CD27 (1:7 PE-conjugated), CD38 (1:30 PE-Cy7 conjugated), IgM (1:100 Cy5-conjugated), CD86 (1:5 APC-conjugated), CD3 (1:7 fluorescein isothiocyanate-conjugated [FITC]), CD56 (1:7 FITC-conjugated), CD19 (1:20 APC-Cy7-conjugated). All antibodies were purchased from BD. After labeling, cells were washed twice in PBS/FBS (2%) and data were acquired with a FACS Canto II (BD). Flow cytometer profiles were analyzed using FACSDiva software (BD). A minimum of 20,000 events were collected per dataset.

For selected experiments the MVs derived from supernatant of $2x10^6$ seeded MSCs grown at confluence were isolated with the procedure described above and added with 5 µl of Annexin V (APC-conjugated, BD) in conjunction with 5µl of vital dye 7-AAD (PerCP-conjugated, BD) in a final volume of 500 µl of Annexin V Binding Buffer 1X (BB1x) according with the manufacture's guideline. After 15 min of incubation in the dark at room temperature, the MV samples were transferred on Troucount tubes (BD) containing calibration beads in order to gate the MVs by morphological parameters (forward scatter FSC-H; side scatter, SSC-H).

MSC-MV cytokine content.

Pelletted MSC-MVs were mixed with Triton X-100 (1% final concentration) and the lysate was assayed with the FluoCytomix Multiple Analyte Detection kit (eBioscience, San Diego, CA) according to the manufacturer instructions. Assayed human cytokines included interferon (IFN)-γ, interleukin (IL)-1β, IL-2, IL-4, IL-5, IL-6, IL-8, IL-10, IL-12 p70, tumor necrosis factor (TNF)-α, TNF-β. MSC-MVs were also

maintained in culture medium at 37°C and cytokine release was measured in medium after 2, 4 and 7 days.

Imaging analysis of MSC-MV association with PBMCs

MVs were isolated from the medium of $2x10^6$ MSCs as described above and labeled with $2.5x10^{-6}$M PKH26 (25) (Sigma, Saint Louis, USA) according to the manufacturer's instructions. The labeled MVs were gently added to PBMCs suspension ($5x10^5$ cells/well) in RPMI plus 10% FBS. After 1h of incubation at 37°C in a humidified atmosphere with 5% $C0_2$, the cell population was washed in PBS and split in two aliquots, both for Flow cytometry and for Confocal Microscopy analysis.

Immunofluorescence analysis. PBMCs incubated with PKH26 labeled MVs were rinsed in PBS, fixed in 4% formaldehyde, blocked with PBS/FBS (5%) for 30 min, and single-labeled with the following monoclonal antibodies: anti-CD86 (1:10), anti-CD3 (1:10) and anti-CD19 (1:10), all conjugated to allophycocyanin (BD), as well as anti-CD56 antibody (1:30) FITC-conjugated (BD).

All antibodies were diluted in PBS/bovine serum albumin (BSA) (1%), and incubated for 1 hour. Negative controls were performed using PBMCs samples without the incubation with MVs, as well as omitting the primary antibody in the staining procedure.

Nuclei were counterstained with 1 µg/ml Hoechst 33342 (Invitrogen, Molecular Probes, OR, USA). After washing in PBS, the samples were mounted with Pro-long Anti-Fade reagent (Invitrogen).

Confocal laser microscopy and image processing analysis. The confocal imaging was performed on Olympus Fluoview FV1000 confocal microscope equipped with FV10-ASW version 2.0 software, Multi Ar (458-488 and 515 nm), 2X He/Ne (543 and 633

nm) and 405-nm diode lasers, using 60X (1.35 NA oil) objective. Optical single sections were acquired with a scanning mode format of 1,024 X 1,024 pixels, with a 207 nm/pixel size, sampling speed of 40 µs/pixel, and 12 bits/pixel images. Fluorochrome unmixing was performed by acquisition of automated-sequential collection of multi-channel images, in order to reduce spectral crosstalk between channels. The pinhole aperture was 1 Airy unit.

Z-reconstruction of serial single optical sections was performed with a scanning mode of 1,024 X 1,024 pixels with an electronic zoom at 2, corresponding to 103 nm/pixel, sampling speed of 20 µs/pixel and Z stack of 0.40 µs/slice. Images were processed using Photoshop software version 9.0 (Adobe Systems Inc., CA).

Statistical analysis

Each experiment was run in duplicate and the mean of the two results was calculated. Data were analysed in terms of medians, minimum and maximum values. A nonparametric analysis of variance (Kruskal-Wallis test) followed by Multiple Comparisons by Mean Ranks was performed to compare quantitative data among group. Linear regression analysis was performed to evaluate dose-response relationships. $p<0.05$ was considered statistically significant.

RESULTS

Co-culture of PBMCs with MSCs

We first investigated the effects of MSCs on B cell viability upon stimulation with CpG. We co-cultured CMFDA labeled PBMCs (C) isolated from n=8 healthy donors with MSCs. After 7 days of incubation, we analyzed the CD19 positive cells by cytometric analysis. A significant inhibition of B cell viability was observed at the MSC/C ratio of 1:20 (Figures 1A, 1D). We next investigated whether co-culture with MSCs affects B cell proliferation and differentiation. After 7 days in the previously described experimental conditions, double-stained CD19 CMFDA and CD19/CD27 cells were gated in flow cytometry analysis. As shown maximum inhibition of B cell proliferation (Figure 1B, 1D) and differentiation (Figure 1C, 1D) were observed at 1:20 MSCs/C ratio.

Effect of MSC-MVs on B cell proliferation and differentiation

MSC-MVs were added to PBMCs after 1 and 24 hours from seeding. Statistically significant inhibition of B cell proliferation was observed in the presence of MSC-MVs (Figure 2A upper panel, 2B). The differentiation of Plasma Cells (PCs) from B lymphocytes was also evaluated by double staining with CD19 and CD27. A strong inhibition of PCs was observed in the presence of MSC-MVs (Figure 2A lower panel, 2C). MSC-MVs also inhibited the production of IgM, IgG and IgA by PBMCs (Figure 3).

Apoptosis

The percentage of Annexin V/7-AAD positive B lymphocytes (approximately 2% of the total B lymphocytes) was not statistically different among cells cultured with medium alone, with CpG alone or with CpG and MSC-MVs both after 4 and after 7 days in culture, indicating that the suppressive effect of MSC-MVs was not associated with B cell death. For the sake of simplicity, only data at day 7 are shown (Figure 4).

Characterization of MSC-MVs

A representative density plot of the MSC-MVs population isolated as described above is shown in Figure 5. MSC-MVs are 7-AAD-negative and express Annexin V.

Dose-dependent effect of MSC-MVs on B lymphocytes

Serial dilutions of the MSC-MVs suspension, obtained as described above, were added to $5x10^5$ PBMC cultures. A linear correlation was found between MSC-MVs concentration and the inhibiting effect on B lymphocytes, both with respect to cell proliferation and differentiation (Figure 6A). A dose-dependent inhibitory effect of MSC-MVs was also observed on IgM, IgG and IgA production (Figure 6B).

Cytokine content of MSC-MVs

Both IL-6 and IL-8 were detectable in MSC-MV lysate and were released in culture medium. Both lysate and culture medium tested negative for IFN-γ, IL-1β, IL-2, IL-4, IL-5, IL-10, IL-12 p70, TNF-α, TNF-β.

Analysis of MSC-MV association with PBMCs

Flow cytometry analysis of PBMCs pre-incubated with PKH26-labeled MSC-MVs revealed that these particles were associated with a subset of CD86/CD19 positive cells corresponding to B lymphocytes. No association of labeled MSC-MVs was found either with CD3 positive cells (corresponding to T lymphocytes) or with CD56 positive cells (corresponding to natural killer [NK] cells) (Figure 7).

In order to further evaluate the association of MSC-MVs with specific cell phenotypes, we performed the immunofluorescence analysis of PBMC samples preincubated or not with labeled MSC-MVs by confocal laser scanning microscopy (Figure 8). A panel of fluorescently labeled antibodies directed to CD3, CD19, CD56 and CD86 molecules was used and the colocalization analysis revealed a consistent association of MSC-MVs with CD19 and CD86 positive cells, whereas no association was observed with CD3 and CD56 positive cells (Figure 9). The analysis of the localisation of red fluorescently labeled MSC-MVs within cells was based on the Z-reconstruction of serial single optical sections of CD19 and CD86 positive cells (Figure 9). The MSC-MVs distribution in the lateral and axial dimensions, visualized by XZ- and YZ-axis projections, confirmed their intracellular localization in the cytoplasm of CD19 and CD86 positive-cells (Figure 9).

DISCUSSION

The immunomodulatory effect of MSCs on B cells is still controversial, and the mechanisms involved are unclear (8,10,22,26,28,30). Because of the documented species differences (23), we will discuss previously published work with human cells only. The role of soluble factors is generally recognized, and it was found to be more

relevant in mediating the effect on B than on T lymphocytes (1). It has been proposed that the conflicting results between different laboratories could derive from differences in the methods used to isolate and characterize MSCs (21). For our studies, we relied on a commercial MSC preparation, which in our hands demonstrated good batch-to-batch reproducibility in the present experimental setup (data not shown). Also, we studied the effect of MSCs in culture with PBMCs rather than with purified B cells, since the former is a more physiological system, including all immune competent cells.

We observed that MSCs exert a strong inhibitory effect on B cell proliferation and differentiation in PBMCs, in agreement with previous reports (8,10,26) but not with others (22,28). Both effects could be fully reproduced with MSC-MVs. MSC-MVs affected also B cell lineage function, as shown by the strong inhibition on immunoglobulin secretion. Also, a linear relationship was observed between MSC-MVs concentration and the inhibition of B cell proliferation and differentiation.

It has been reported that the suppressive effect of MSCs on B cells was still present when separating PBMCs and MSCs by a permeable membrane (1,10). However, such inhibition was absent (10) or only partial (1) when using MSC supernatant. It was thus hypothesized that the inhibitory effect of MSCs required cell-to-cell contact or the release of paracrine signals from B cells in order to be fully expressed (10). However, the present results show that MSCs effect on both B cell proliferation and differentiation can be fully reproduced by MSC-MVs in a dose-dependent fashion. We thus hypothesize that the concentration of MSC-MVs in the microenvironment surrounding B cells could determine the degree of inhibition and could play a role as regulatory factor *in vivo*, since MSCs migrate to inflammation sites (11). Experimental

differences affecting MSC-MVs availability to B cells can probably explain previous conflicting results.

In order to evaluate whether other cell types present in PBMCs were involved in the observed phenomenon, we labeled MSC-MVs with a fluorescent dye and found them to be associated only with stimulated B cells, both by FACS analysis and at confocal microscopy.

These data suggest that the suppressive effect of MSCs on B cells is largely mediated by MV release. The role of MVs as conveyors of the immune response has been demonstrated in several pathways, involving all immune cell phenotypes (27). MVs derived by MSCs have been previously described as possible mediators of the antiapoptotic (13) and proregenerative effect (3,15) associated with MSC administration. However, their role in mediating MSC-induced B cell suppression was not described so far. We found that MSC-MVs contain IL-6 and IL-8. IL-6 production by MSCs has been described previously (22). Clearly, the identification of these cytokines in MSC-MVs don't allow to draw any immediate hypothesis on the mechanisms underlying their immunosuppressive effect. Even if in our experimental setup these particles were found to be preferentially associated with stimulated B cells, the observed effect could result from an interplay with other cell types present in PBMCs. In order to characterize the MSC-MVs preparations, we used Annexin V binding as a morphological/functional marker. It is known (14) that due to phospholipid asymmetry, some MVs express Phosphatylserine (PS) on the outer surface, and thus bind Annexin V. In our experience approximately 22% of MSC-MVs bound Annexin V in agreement with Connor et al (9). The biological significance, if any, of these different MV populations is presently unknown.

MSCs were reported to have both inhibitory (8,10,26) and stimulatory (22,28) effects on B cell proliferation, differentiation and antibody production. Under some conditions, MSCs can function as antigen presenting cells, thus enhancing the immune response (6). In one study involving interaction with B cells, MSCs were found to exhibit opposite effects (i.e. either inhibitory or stimulatory) depending on the magnitude of the stimulus used to trigger the B cells or on the different cell donors (22). Such unpredictable outcomes raise concern on the possibility to control the effect of administered MSCs in complex autoimmune disorders. MSC-MVs could possibly represent a safer and more reproducible therapeutic tool than MSCs. The clinical use of MVs was found to be both feasible and safe in phase I trials involving MVs derived from dendritic cells for immunotherapy of advanced cancer (12,20). Clearly, additional studies are needed to explore the role of MSC-MVs as modulators of immune response before they can be proposed for clinical use in place of the parent cells.

ACKNOWLEDGEMENTS

The work was supported by the Italian Ministry of Health. We thank Paolo Parini for help with the statistical analysis, Rita Carsetti and Ezio Giorda for FACS analysis.

CONFLICT OF INTEREST

The authors declare no conflict of interest in the conduction of this study.

REFERENCES

1. Augello, A.; Tasso, R.; Negrini, S. M.; Amateis, A.; Indiveri, F.; Cancedda, R.; Pennesi, G. Bone marrow mesenchymal progenitor cells inhibit lymphocyte proliferation by activation of the programmed death 1 pathway. Eur. J. Immunol. 35:1482-1490; 2005.
2. Beyth, S.; Borovsky, Z.; Mevorach, D.; Liebergall, M.; Gazit, Z.; Aslan, H.; Galun, E.; Rachmilewitz, J. Human mesenchymal stem cells alter antigen-presenting cell maturation and induce T-cell unresponsiveness. Blood 105:2214-2219; 2005.
3. Bruno, S.; Grange, C.; Deregibus, M. C.; Saviozzi, S.; Collino, F.; Bussolati, B.; Tetta, C.; Camussi, G. Mesenchymal stem cell-derived microvesicles protect against acute tubular injury. J. Am. Soc. Nephrol. 20:1053-1067; 2009.
4. Caimi, P. F.; Reese, J.; Lee, Z.; Lazarus, H. M. Emerging therapeutic approaches for multipotent mesenchymal stromal cells. Curr. Opin. Haematol. 17:505-513; 2010.
5. Camussi, G.; Deregibus, M. C.; Bruno, S.; Cantaluppi, V.; Biancone, L. Exosomes/microvesicles as a mechanism of cell-to-cell communication. Kidney Int. 78:838-848; 2010.
6. Chan, J. L.; Tang, K. C.; Patel, A. P.; Bonilla, L. M.; Pierobon, N.; Ponzio, N. M.; Rameshwar, P. Antigen-presenting property of mesenchymal stem cells occurs during a narrow window at low levels of interferon-gamma. Blood 107:4817-4824; 2006.
7. Collino, F.; Deregibus, M. C.; Bruno, S.; Sterpone, L.; Aghemo, G.; Viltono, L.; Tetta, C.; Camussi, G. Microvesicles derived from adult human bone marrow

and tissue specific mesenchymal stem cells shuttle selected pattern of microRNAs. PloS One 5:e11803; 2010.

8. Comoli, P.; Ginevri, F.; Maccario, R.; Avanzini, M. A.; Marconi, M.; Groff, A.; Cometa, A.; Cioni, M.; Porretti, L.; Barberi, W.; Frassoni, F.; Locatelli, F. Human mesenchymal stem cells inhibit antibody production induced in vitro by allostimulation. Nephrol. Dial. Transplant. 23:1196-1202; 2008.
9. Connor, D. E.; Exner, T.; Dang Fung Ma, D.; Joseph, J. E. The majority of circulating platelet-derived microparticles fail to bind annexin V, lack phospholipid-dependent procoagulant activity and demonstrate greater expression of glycoprotein Ib. Thromb. Haemost. 103:1044-1052; 2010.
10. Corcione, A.; Benvenuto, F.; Ferretti, E.; Giunti, D.; Cappiello, V.; Cazzanti, F.; Risso, M.; Gualandi, F.; Mancardi, G. L.; Pistoia, V.; Uccelli, A. Human mesenchymal stem cells modulate B-cell functions. Blood 107:367–372; 2006.
11. da Silva Meirelles, L.; Caplan, A. I.; Nardi, N. B. In search of the in vivo identity of mesenchymal stem cells. Stem Cells 26:2287-2299; 2008.
12. Escudier, B.; Dorval, T.; Chaput, N.; André, F.; Caby, M. P.; Novault, S.; Flament, C.; Leboulaire, C.; Borg, C.; Amigorena, S.; Boccaccio, C.; Bonnerot, C.; Dhellin, O.; Movassagh, M.; Piperno, S.; Robert, C.; Serra, V.; Valente, N.; Le Pecq, J. B.; Spatz, A.; Lantz, O.; Tursz, T.; Angevin, E.; Zitvogel, L. Vaccination of metastatic melanoma patients with autologous dendritic cell (DC) derived exosomes: results of the first phase I clinical trial. J. Transl. Med. 3:10-17; 2005.
13. Gatti, S.; Bruno, S.; Deregibus, M. C.; Sordi, A.; Cantaluppi, V.; Tetta, C.; Camussi, G. Microvesicles derived from human adult mesenchymal stem cells

protect against ischaemia-reperfusion-induced acute and chronic kidney injury. Nephrol. Dial. Transplant. 26:1474-1483; 2011.

14. Gyorgy, B.; Szabò, T. G.; Pasztòi, M.; Pàl, Z.; Misjàk, P.; Aradi, B.; Làszlò, V.; Pàllinger, E.; Pap, E.; Kittel, A.; Nagy, G.; Falus, A.; Buzàs, E. I. Membrane vesicles, current state of the art: emerging role of extracellular vesicles. Cell. Mol. Life Sci. 68:2667-2688; 2011.
15. Herrera, M. B.; Fonsato, V.; Gatti, S.; Deregibus, M. C.; Sordi, A.; Cantarella, D.; Calogero, R.; Bussolati, B.; Tetta, C.; Camussi, G. Human liver stem cell-derived microvesicles accelerate hepatic regeneration in hepatectomized rats. J. Cell. Mol. Med. 14:1605-1618; 2010.
16. Kebriaei, P.; Robinson, S. Treatment of graft-versus-host-disease with mesenchymal stromal cells. Cytotherapy 13:262-268; 2011.
17. Krampera, M.; Glennie, S.; Dyson, J.; Scott, D.; Simpson, E.; Dazzi, F. Bone marrow mesenchymal stem cells inhibit the response of naïve and memory antigen-specific T cells to their cognate peptide. Blood 101:3722-3729; 2003.
18. Lamparski, H. G.; Metha-Damani, A.; Jenq-Yuan, Y.; Le Pecq, J. B. Production and characterization of clinical grade exosomes derived from dendritic cells. J. Immunol. Methods 270:211-226; 2002.
19. Meirelles Lda, S.; Fontes, A. M.; Covas, D. T.; Caplan, A. I. Mechanisms involved in the therapeutic properties of mesenchymal stem cells. Cytokine Growth Factor Rev. 20:419-427; 2009.
20. Morse, M. A.; Garst, J.; Osada, T.; Khan, S.; Hobeika, A.; Clay, T. M.; Valente, N.; Shreeniwas, R.; Sutton, M. A.; Delcayre, A.; Hsu, D. H.; Le Pecq, J. B.; Lyerly, H. K. A phase I study of dexosome immunotherapy in patients with advanced non-small cell lung cancer. J. Transl. Med. 3:9-17; 2005.

21. Ozaki, K.; Sato, K.; Oh, I.; Meguro, A.; Tatara, R.; Muroi, K.; Ozawa, K. Mechanisms of immunomodulation by mesenchymal stem cells. Int. J. Haematol. 86:5-7; 2007.
22. Rasmusson, I.; Le Blank, K.; Sundberg, B.; Ringdén, O. Mesenchymal stem cells stimulate antibody secretion in human B cells. Scand. J. Immunol. 65:336-343; 2007.
23. Ren, G.; Su, J.; Zhang, L.; Zhao, X.; Ling, W.; L'huillie, A.; Zhang, J.; Lu, Y.; Roberts, A.I.; Ji, W.; Zhang, H.; Rabson, A. B.; Shi, Y. Species variation in the mechanisms of mesenchymal stem cell-mediated immunosuppression. Stem Cells 27:1954-1962; 2009.
24. Sattler, C.; Steinsdoerfer, M.; Offers, M.; Fischer, E.; Schierl, R.; Heseler, K.; Däubener, W.; Seissler, J. Inhibition of T cell proliferation by murine multipotent mesenchymal stromal cells is mediated by CD39 expression and adenosine generation. Cell Transplant. 20:1221-1230; 2011.
25. Sheehy, M. E.; McDermott, A. B.; Furlan, S. N.; Klenerman, P.; Nixon, D. F. A novel technique for the fluorometric assessment of T lymphocyte antigen specific lysis. J. Immunol. Methods 249:99-110; 2001.
26. Tabera, S.; Perez-Simon, J.; Diez-Campelo, M.; Sanchez-Abarca, L. I.; Bianco, B.; Lopez, A.; Benito, A.; Ocio, E.; Sanchez-Guijo, F. M.; Canino, C.; San Miguel, J. F. The effect of mesenchymal stem cells on the viability, proliferation and differentiation of B-lymphocytes. Haematologica 93:1301-1309; 2008.
27. Théry, C.; Ostrowski, M.; Segura, E. Membrane vesicles as conveyors of immune responses. Nat. Rev. Immunol. 9:581-593; 2009.

28. Traggiai, E.; Volpi, S.; Schena, F.; Gattorno, M.; Ferlito, F.; Moretta, L.; Martini, A. Bone marrow-derived mesenchymal stem cells induce both polyclonal expansion and differentiation of B cells isolated from healthy donors and systemic lupus erythematosus patients. Stem Cells 26:562-569; 2008.
29. Valadi, H.; Ekström, K.; Bossios, A.; Sjöstrand, M.; Lee, J. J.; Lötvall, J. O. Exosome-mediated transfer of mRNAs and microRNAs is a novel mechanism of genetic exchange between cells. Nat. Cell Biol. 9:654-669; 2007.
30. Yagi, H.; Soto-Gutierrez, A.; Parekkadan, B.; Kitagawa, Y.; Tompkins, R. G. ; Kobayashi, N.; Yarmush, M. L. Mesenchymal stem cells: Mechanisms of immunomodulation and homing. Cell Transplant. 19:667-679; 2010.
31. Zhao, S.; Wehner, R.; Bachmann, M.; Schimtz, M. Immunomodulatory properties of mesenchymal stromal cells and their therapeutic consequences for immune-mediated disorders. Stem Cells Dev. 19:607-614; 2010.

LEGENDS TO FIGURES

Figure 1. Co-culture of CpG-stimulated PBMCs with MSCs. A-C) Representative density plots. Cytometric analysis was performed by morphological parameter (forward scatter, FSC-H) of chloromethylfluorescein diacetate (CMFDA) labeled peripheral blood mononuclear cells (PBMCs) (C) or PBMCs after co-culture with mesenchymal stromal cells (MSCs) (MSCs/C) at ratio 1:20, 1:50 and 1:100 respectively. A) Positive CD19 cells were gated in R1 from PBMCs cultured with or (C) without MSCs. B) In the upper left quadrant Q1 the percentage of CD19/CMFDA positive cells is shown for PBMCs cultured with or (C) without MSCs. C) Double positive CD19/CD27 Plasma cells (PCs) are shown for PBMCs cultured with or (C) without MSCs. D) Inhibition of viability, proliferation and differentiation of CpG-stimulated B cells in PBMCs cultured with or (C) without MSCs. Graphs show individual data and medians of 3 independent experiments.

Figure 2. Effect of MSC-MVs on CpG-stimulated PBMCs

A**)** Representative density plots of cytometric analysis of CMFDA labeled PBMCs cultured in medium alone or with CpG or with MSC-membrane vesicles (MVs) and CpG. Lymphocytes were gated in Q1 by morphological parameters (FSC-H; SSC-H) as living cells (left). They were subsequently analyzed either for the proliferation rates by CMFDA/CD19 staining (right, upper panel) or for the differentiation stage of Plasma Cells (PCs) by selecting CD19/CD27 positive events (right, lower panel). B) Inhibition of proliferation of CMFDA/CD19 positive lymphocytes from a culture of PBMCs cultured in medium alone or with CpG or with MSC-MVs and CpG. C) Inhibition of differentiation of CD19/CD27 positive plasma cells (PCs) from a culture

of PBMCs cultured in medium alone or with CpG or with MSC-MVs and CpG. Graphs show individual data and medians of 4 independent experiments.

Figure 3. Inhibition of immunoglobulin production in CpG-stimulated PBMCs after incubation with MSC-MVs. ELISA assay of supernatants from a culture of PBMCs cultured in medium alone or with CpG or with MSC-MVs and CpG. Graphs show individual data and medians of IgM, IgG or IgA concentrations (10^2 ng/ml) in 4 independent experiments.

Figure 4. Detection of apoptosis. Annexin V/7-amino-actinomycin (7-AAD) analysis of proliferating CD19 positive cells maintained for 7 days in medium alone, with CpG or treated with MSC-MVs plus CpG. Graphs show individual data and medians of 3 independent experiments.

Figure 5. Flow cytometry analysis of MSC-MVs. Representative scatter plot obtained by flow cytometry of MSC-MVs. A) The MSC-MVs were gated using size calibration beads to define the proper gate of events within 0.5-1µm dimensions. B) MSC-MVs derived from the gate shown in A were identified in quadrant Q4 by Trucount beads (P1), Annexin V positivity and 7-AAD negativity. The percentage of Annexin V positive/7-AAD negative MSC-MVs is indicated in Q4.

Figure 6. Dose-dependent inhibitory effect of MSC-MVs on B lymphocytes. Panel A: inhibition of proliferation (left) and differentiation (right) of CpG-stimulated PBMCs after culture with undiluted MSC-MVs and at 1:3–1:6 dilutions. Panel B:

immunoglobulin ELISA assay of supernatants from a culture of PBMCs alone (not shown) or incubated with MSC-MVs, 1:3 or 1:6 dilutions. A significant dose-dependent inhibition of IgM, IgG and IgA production was observed. The results were obtained from 4 independent experiments.

Figure 7. Fluorescence-activated cell sorting (FACS) analysis of the association between PKH26 labeled MSC-MVs and selected cell phenotypes in CpG-stimulated PBMCs. A) Density Plots of CD3+, CD86+ and double negative lymphocytes (DNeg), selected in 3 different gates. B) Histograms plots of fluorescence intensity (IF) of CD3-FITC, CD86-APC positive gated lymphocytes analyzed before (upper panel) or after incubation with PKH26 labeled MSC-MVs (lower panel). C) Density Plots of CD56+, CD19+ and double negative lymphocytes (DNeg), selected in 3 different gates. D) Histograms plots of IF of CD56-FITC, CD19-APC-Cy7 positive gated lymphocytes analyzed before (upper panel) or after incubation with PKH26 labeled MSC-MVs (lower panel). After incubation with PKH26 labeled MSC-MVs the levels of IF (plotted values in the upper right quadrant) increases in CD86+ cells (IF=1,244 versus basal level IF=78) and in CD19+ cells (IF=1,424 versus basal level IF=123) respectively.

Figure 8. Confocal microscopy of the association between PKH26 labeled MSC-MVs and selected cell phenotypes in CpG-stimulated PBMCs. PBMCs immunolabeled with antibodies against CD3, CD19 and CD86 conjugated to allophycocyanin (pseudocoloured in green), and FITC-conjugated CD56 (green), with (right panel) and without (left panel) incubation with PKH26 labeled-MVs (red). Nuclei

were counterstained with Hoechst. MSC-MVs were only associated with CD19 (arrowheads) and CD86 (arrows) positive cells. Magnification bar: 10 μm.

Figure 9. Confocal microscopy analysis of microphotograps of Z-reconstruction. The analysis of microphotograps of Z-reconstructions (a, d) performed by confocal laser scanning microscopy of CpG-stimulated PBMCs incubated with PKH26 positive-MVs and stained with anti-CD19 (a-c) and anti-CD86 (d-f) antibodies. XZ and YZ-axis projections (b-c, e-f) obtained from multiple consecutive optical sections, showing the intracellular localization of red fluorescently labeled MVs in CD19 (c, in green) and CD86 (f, in green) positive cells**.** Nuclei were stained with Hoechst. Magnification bars: 5 μm (a, d) and 2 μm (b-c, e-f).

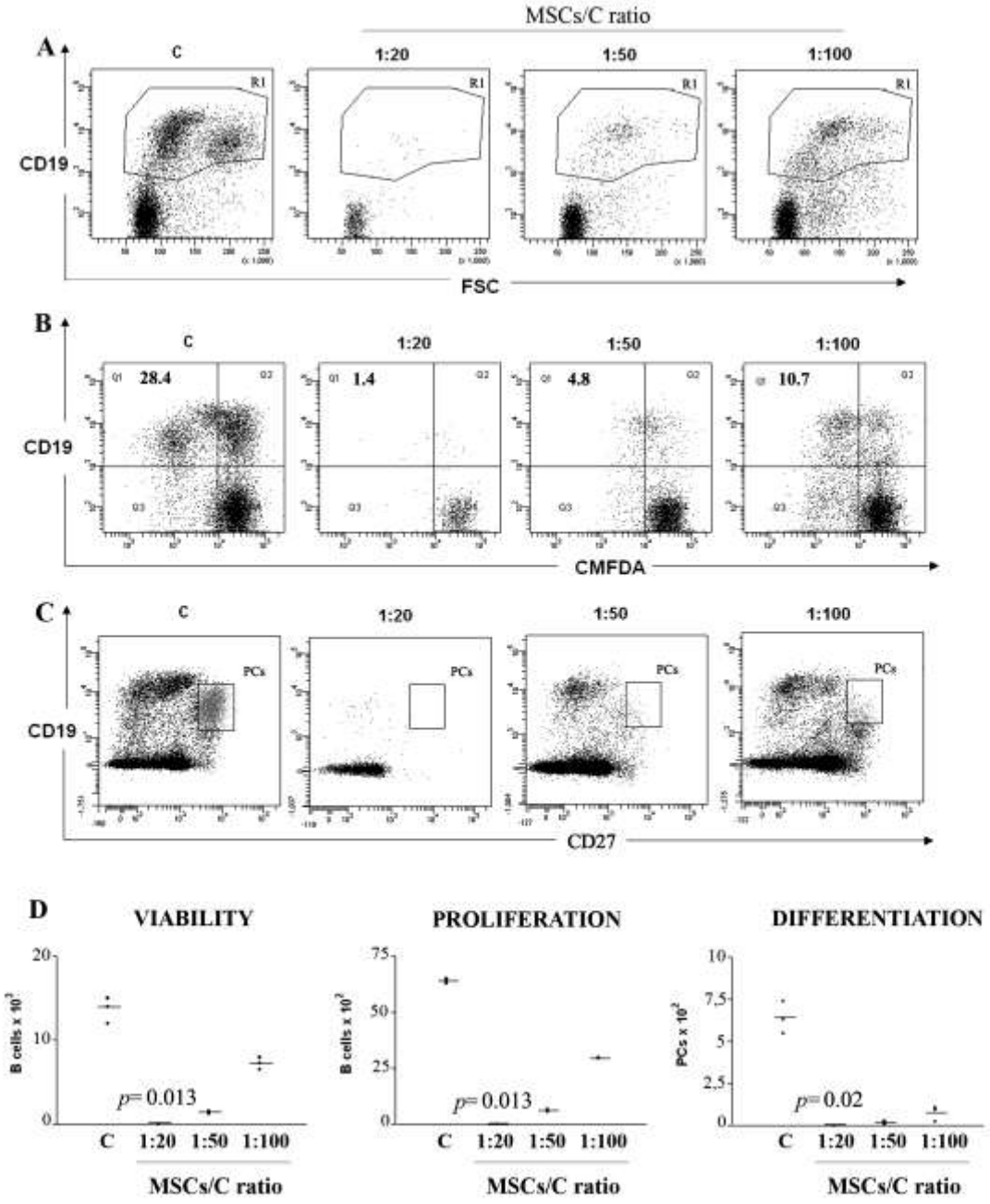

Figure 1

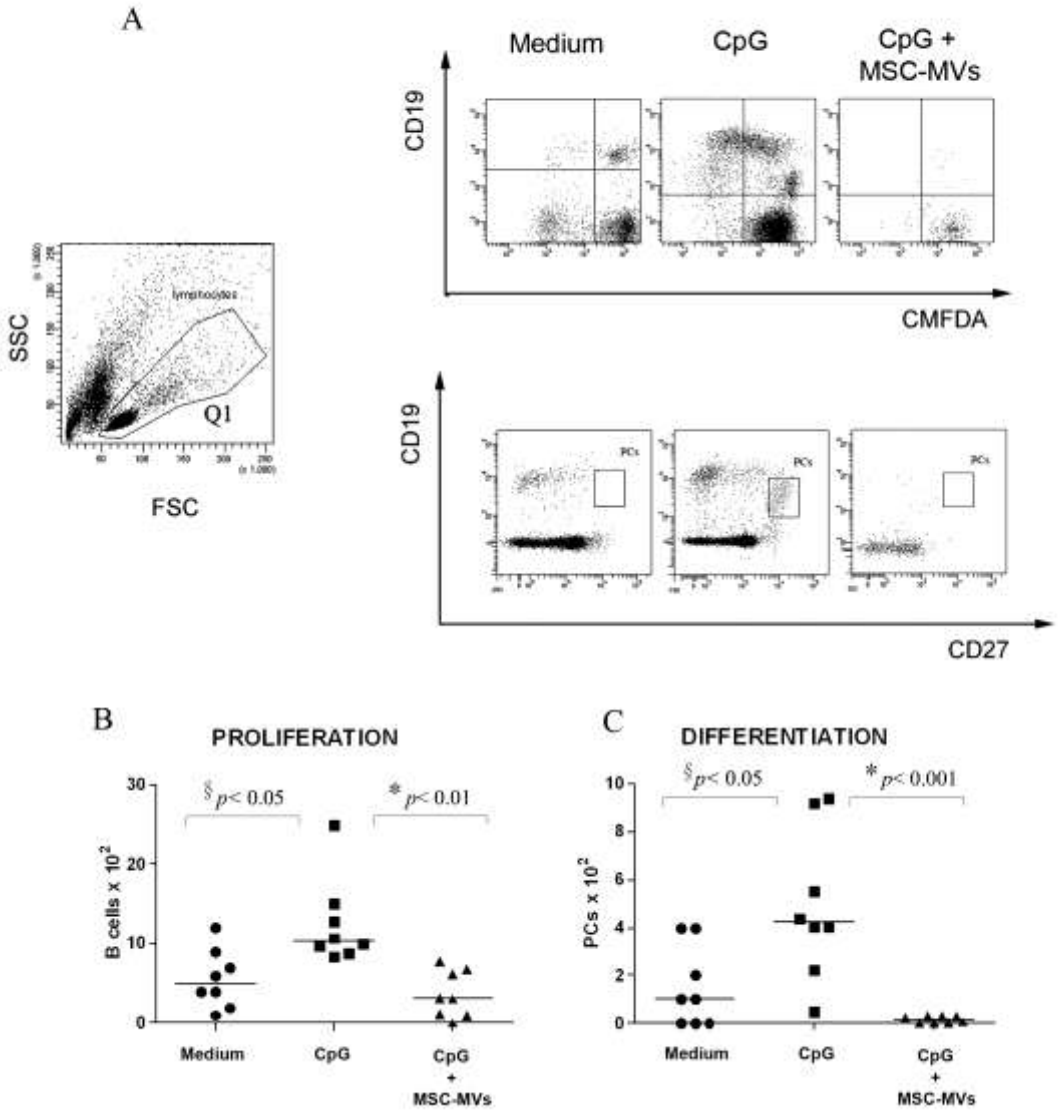

Figure 2

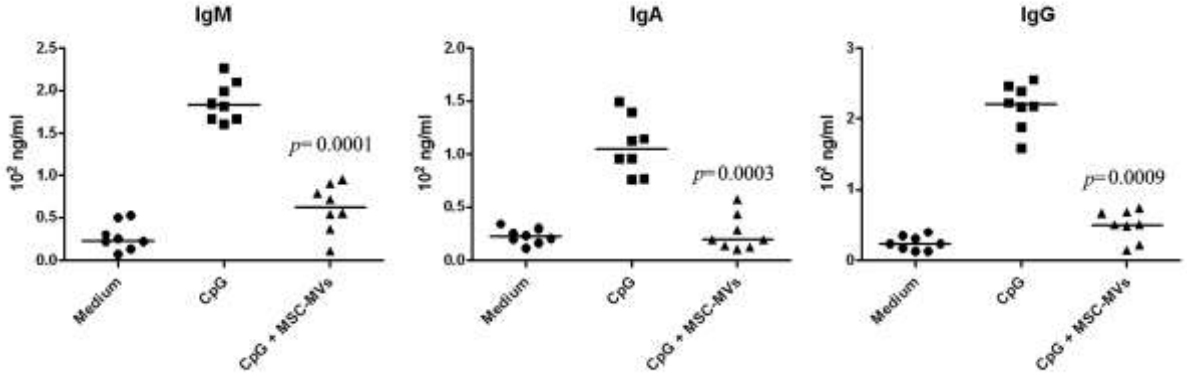

Figure 3

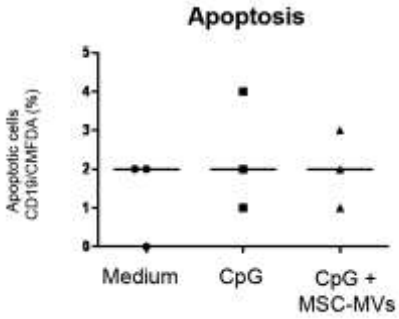

Figure 4

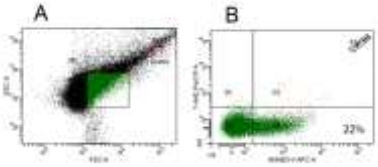

Figure 5

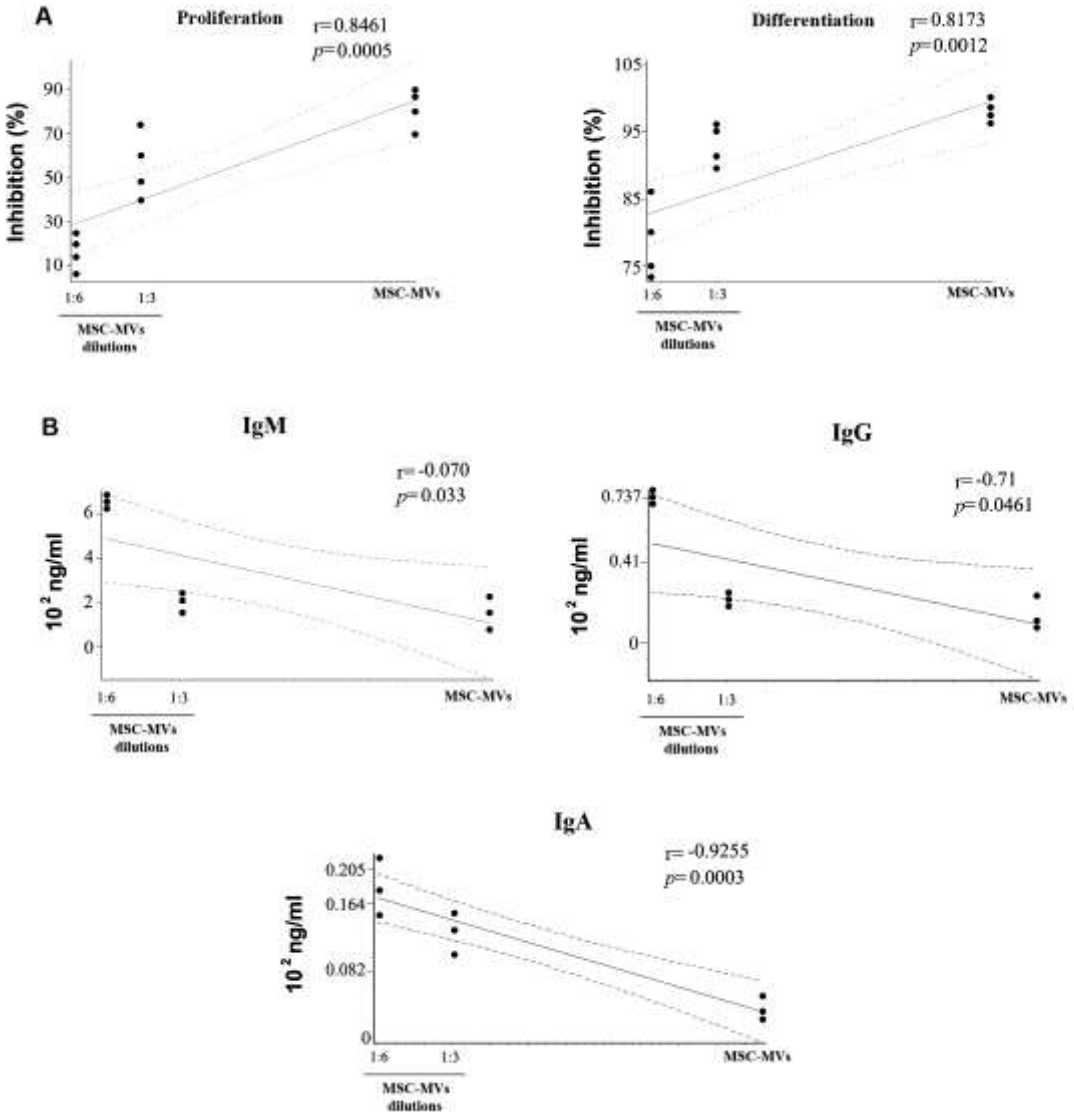

Figure 6

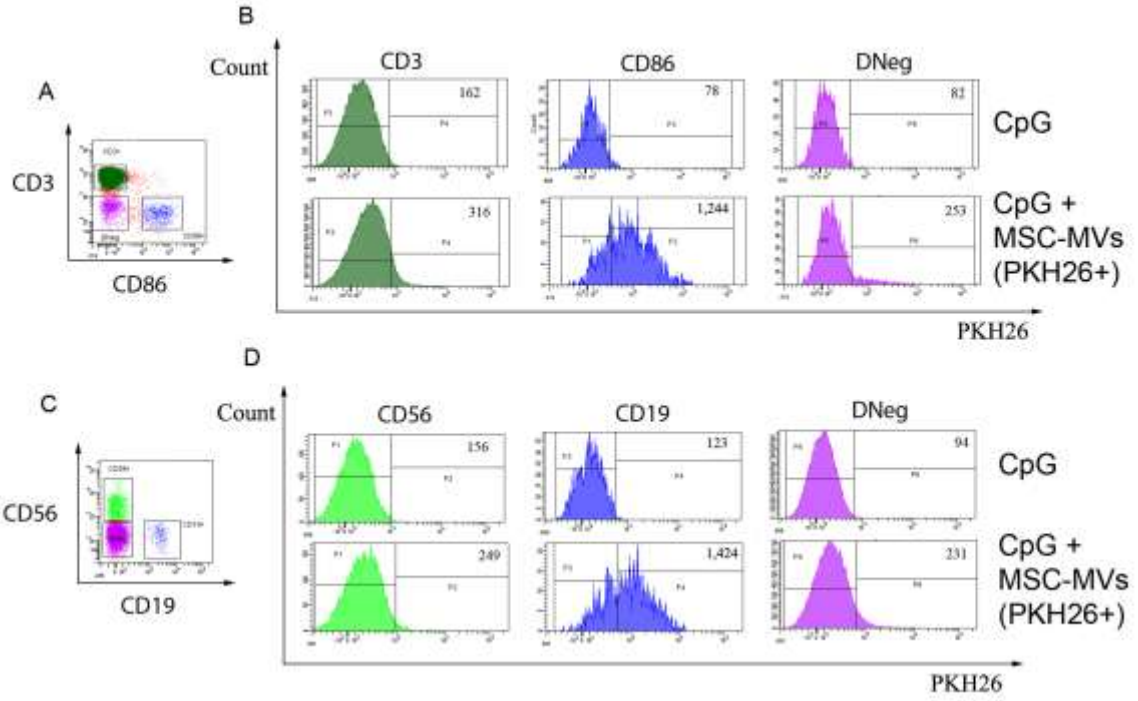

Figure 7

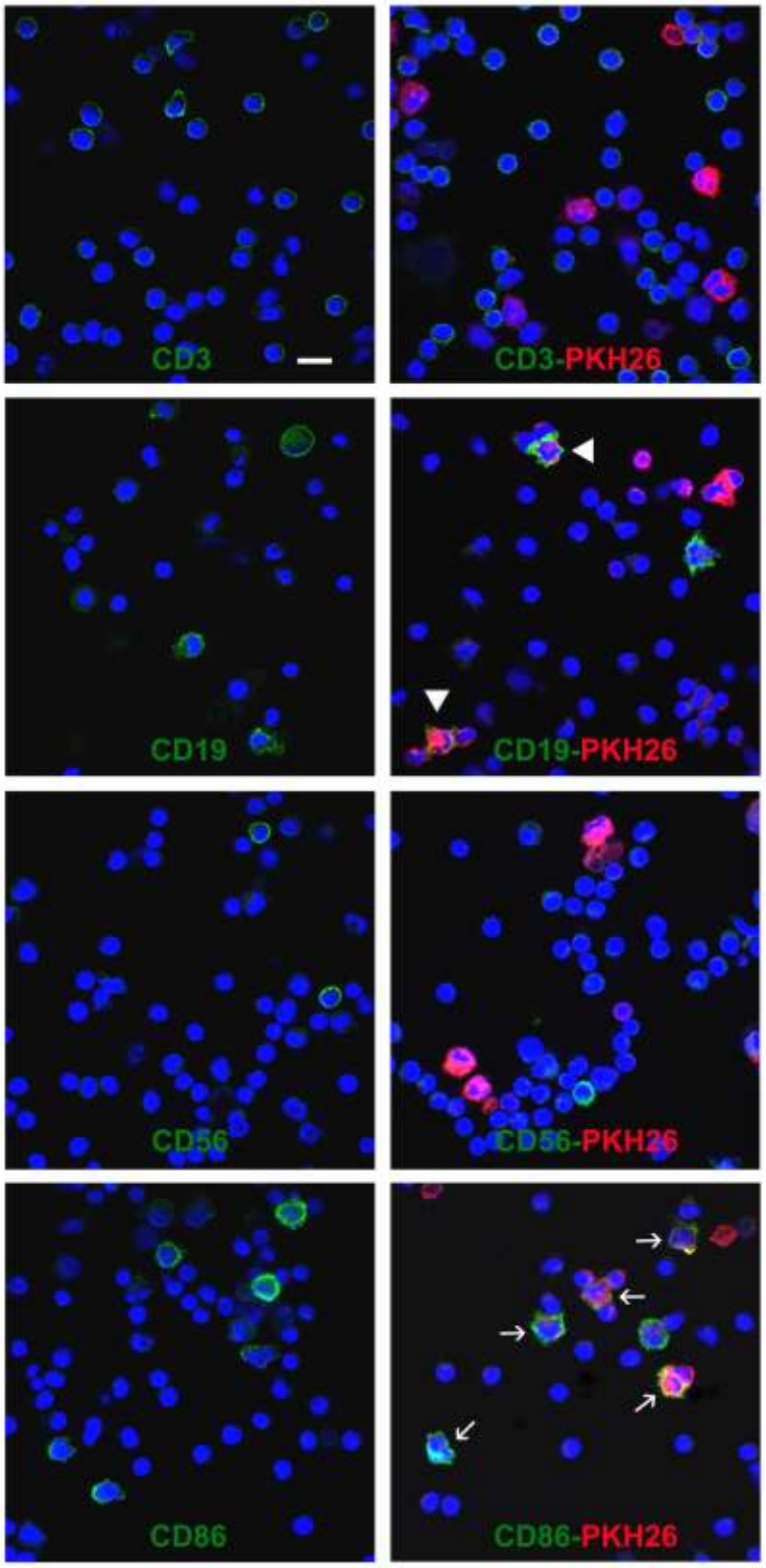

Figure 8

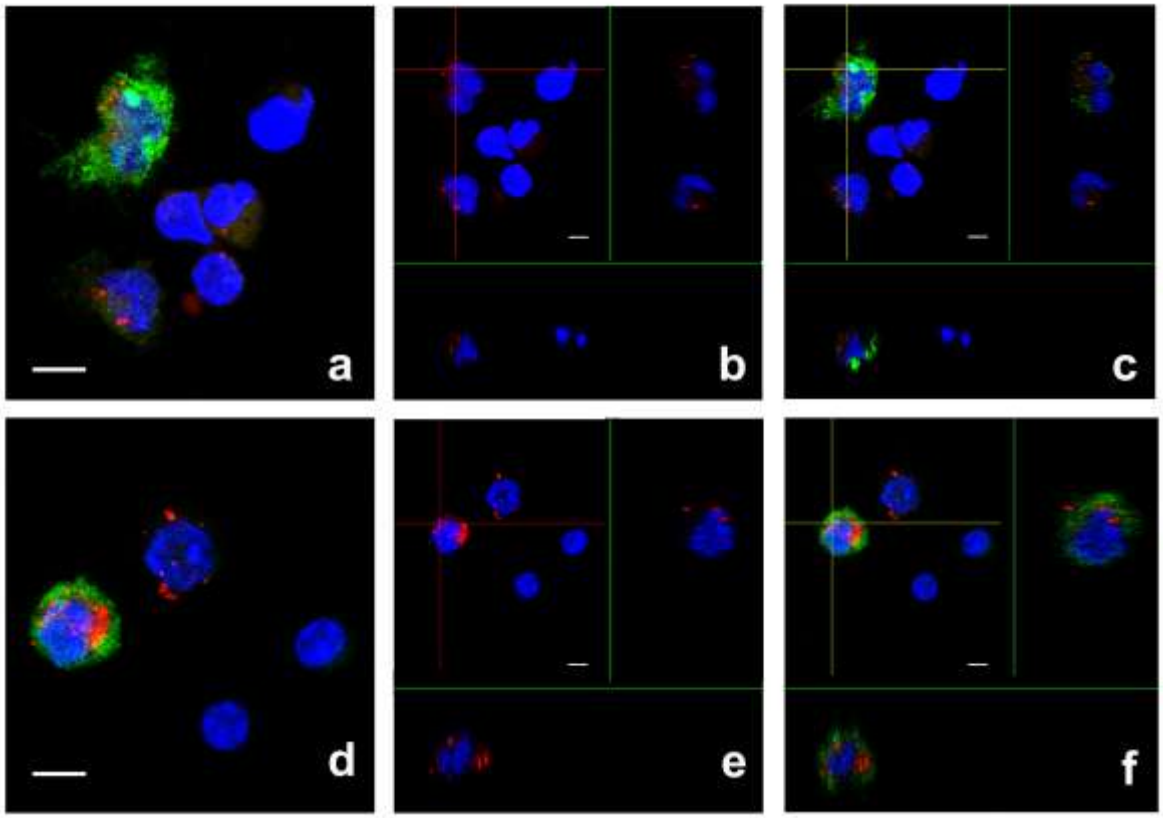

Figure 9